



Aerodynamics Analysis and Range Enhancement Study of 81mm Mortar Shell (French Design)

Roman Kalvin^{1,3}, Juntakan Taweekun^{2,*}, Muhammad Waqas Mustafa³, Saba Arif¹

¹ Energy Technology Program, Faculty of Engineering, Prince of Songkla University Hat Yai, Thailand

² Department of Mechanical Engineering, Faculty of Engineering, Prince of Songkla University Hat Yai, Songkhla 90112, Thailand

³ Department of Mechanical Engineering, University of Wah, Wah Cantt. Pakistan

ARTICLE INFO

Article history:

Received 4 February 2021

Received in revised form 10 June 2021

Accepted 13 June 2021

Available online 2 July 2021

Keywords:

Solidworks 2016; CFD; ANSYS Fluent 16.0; 81mm Mortar Shell (French Design)

ABSTRACT

The aim of this research is performing the Computational Fluid Dynamics (CFD) analysis of 81mm Mortar Shell (French Design). The analysis is performed using ANSYS Fluent Software on three different Mach numbers (0.72, 0.76, and 0.84) and results are compared with existing design of 81mm HE M57D A2 Mortar. The drag coefficient of new modified design is found to be less than the existing model. The range of mortar shell is increased by 271 meters because of low drag coefficient with 5.96% percent increase in range and 15.73% decrease in drag coefficient value. Parabolic type; light weighted material fuze casing applied over the existing fuze will result in increase in aerodynamics, range enhancement and drag coefficient reduction. Weight optimization by using lighter material for mortar components and increasing the muzzle velocity can also increase flight duration of the projectile and increase its range. The analysis on 81mm Mortar Shell is a part of range enhancement study to overcome the short fall in required range of mortar shells.

1. Introduction

The last few decades have witnessed vast research on new types of heat transfer fluids, namely nanofluids [1]. Nanofluid is a fluid that contains nanometer-sized solid particles. The nanofluid was introduced by Choi and it has been proven to give better heat transfer efficiency compared to conventional fluids [2]. Detailed reviews on the physical and thermal properties of nanofluids can be seen in review papers by several authors [3-5].

A nanofluid can be produced by dispersing metallic or non-metallic nanoparticles or nanofibers with a typical size of less than 100 nm in a base liquid. French weapons engineer Edgar William Brandt is credited for assistance and development in the field of mortars and projectiles that encompasses different mortar systems such as 60mm, 81mm and 120mm mortars. 81mm Mortar Shell is a smooth bore, medium weight, muzzle loading and with high angle of fire weapon. 81mm Mortar Shell is used with Hotchkiss-Brandt mortars of types: MO-81-61 C and MO-81-61 L short and

* Corresponding author.

E-mail address: jantakan.t@psu.ac.th

long barrel respectively. It is employed to bestow indirect fire assistance to light infantry, air assault and air born units by providing both fragmentation and blast effect. M252 Mortars are used by U.S., U.K. and Canada due to its extended range and lethality. In the late 2014, a lighter version of M252 was produced; due to reduction in weight by using a lighter material, named as M252A1, it replaced all U.S. Army Mortars. Afterwards, another version was produced that was lighter in weight and incorporated a 4x magnification sight with a new cooling system which was named as M252A2. For the enhancement of range, the aerodynamic design optimization of 81mm Mortar Shell was studied in 1994-1995 by DSTO Australia. The limitation in range enhancement was muzzle velocity constraint that did not change due to barrel strength limitation. Wind tunnel testing was conducted on a scaled model (80%) by using a wind tunnel (cross section of 380mm x 360mm) as well as using different types of fuzes and fins. Boyer studied aerodynamic properties specially spin, drag, yaw and roll properties of 60mm T24 mortar shell under transonic range fire testing [1]. Test was conducted fins less mortar, fins with two and four degree cants respectively and evident information regarding drag; in range standard deviation in drag, yaw moments; poor determination of yaw damping coefficients and inconsistencies in yaw moment because of manufacturing variation were discussed. Odom *et al.*, revised the 155mm howitzer firing tables and incorporate drag characteristics and performance of M107 shell under transonic range measurements [2].

Sturek *et al.*, predict the aerodynamic performance and validate the code based on Navier-Stokes computational techniques for both spin, fin and flare stabilized projectiles at supersonic velocity as well as gave insight to the need of supercomputer in this field [3]. Akcay *et al.*, developed a universal external ballistic trajectory model for unguided projectiles [4]. Maclaurin Series based model considers the aerodynamics as well as height affects above sea level for several different calibers of projectiles. Results were compared with trajectory radar measurements and the modified point mass trajectory model. Damljanovic *et al.*, compared and analyzed CFD and experimental results of aerodynamic coefficients and axial force using numerical flow visualization and Schlieren method [5]. 17% and 5% difference were observed in axial force at Mach 2 and Mach 4 respectively and none in normal force and pitching moment coefficients. Moreover, flow images obtained using FLUENT were analyzed and supports experimental results as well. Sagat *et al.*, calculated and discussed drag and lift coefficient by neglecting model support and simplifying assumptions for the sole purpose of correction in predicting full scale performance at an angle of attack range from 0-20 degrees with a max. velocity of 15 m/s [6]. At the end CFD analysis and experimental results at low Reynolds number were compared where pressure coefficient were seen to be minimum on upper and lower surface at high and low angle of attack respectively. As well as greater pressure distribution than that of incoming flow stream was observed on the lower side of the airfoil.

Li *et al.*, analyzed the aerodynamics of tail fin-stabilized projectile under four degree of freedom at flight condition (M) 0.6 and angle of attack from -60 to 60 degrees using CFD, MATLAB/Simulink and low low-speed wind tunnel [7]. Result comparison of CFD and revised Karman-Tsien experimental data showed excellent performance attributes of projectiles such as lift, drag and moment coefficients at an angle of attack from -60 to 60 degrees. These analyses also gave insight to design aerodynamic system to simulate flight trajectories, analyze and compare flow fields by reducing cost of field testing. Parab *et al.*, determined the aerodynamics lift and drag coefficient of automobiles using ANSYS 14.5 in order to reduce the testing time and R&D cost of manufacturers [8]. Results of steady state simulations were compared and verified using transient simulation and a 34% decrease and 5% increase in lift and drag coefficients were observed at by the addition of 8 degree diffuser to the original model.

Hassan *et al.*, concentrated on aerodynamic aspects of racing cars and modified rear under body and exhaust direction thereby found 22.13% and 9.5% reduction in drag coefficient [9]. Intensity of negative pressure area at the rear end of car is also evident which could be minimized for subsequent drag reduction. Lia *et al.*, analyzed a tail fin-stabilized projectile with two different shapes under four degree of freedom, angle of attack -8 to 8 degrees and Mach 0.6 using CFD, MATLAB/Simulink and low speed wind tunnel testing [10]. Both the design shows an excellent aerodynamics while the improved design had an increased range of 26.83% to that of original prototype.

Doig *et al.*, analyzed projectile behavior by using CFD simulation, wind tunnel and synergy live range fire testing at Mach 0.9, Mach 1.1 and Mach 1.2 [11]. It was observed that normal force, drag force and pitching moment change predictably at Mach 0.9. Although basic features were captured by RANS but it was recommended to use LES based methodology to take into account shock influence / boundary-layer interaction and wake behavior in future. Chaurasiya *et al.*, did analysis with 22.22 m/s flow velocity on Audi car model R8 [12]. Simulation of vortex shedding, flow separation, drag and lift coefficients using commercial CFD were done and validated using experimental results. Solidworks 2015, GAMBIT 2.4.6, ANSYS Fluent 17.0 and Tec plot 360 were used for CAD Design, Meshing, CFD Solver and Post Processing respectively. Results of 2D analysis obtained were near to experimental results but the result may vary in 3D analysis which was not done because of time consumption.

Fedaravicius *et al.*, solved several problems in mortar design simulator. Internal and external ballistics of two masses were solved as well as drag force was also determined [13]. Sahu and Heavey studied flow control of after body region at subsonic and supersonic speeds using advanced scalable unstructured flow solver [14]. For time accurate unsteady and steady flow simulations of fields high parallel efficiency was achieved. Moments and forces were affected even at zero degree attack angle due to substantially alter of flow field near the base and jet. There by gave insight to flow field interaction with jets and lead to improved design of projectiles and accurate flight trajectories prediction. Zhang *et al.*, studied finned smart bullet (FSB) to generate asymmetric pressure distribution [15]. Thereby providing aerodynamic control moments and forces. CFD simulations were performed to find out the mass centre (MC) position in order to provide a stable flight and gave insight to achieve flight dynamic control.

As from the literature it was observed that there was not much study carried out on drag calculation via CFD based analysis over artillery shells. As CFD based models gives insight to estimate drag and range calculation and minimize cost of research. This research focus on the aerodynamic CFD based analysis of 81mm Mortar Shell with an aim to find drag coefficient and range estimation by developing CFD model through which comparative study of current design with previous design could be done.

2. Research Methodology

The 81mm mortar (French Modified) model was designed using SOLIDWORKS. 3D model of the 81mm mortar was exported onto the ANSYS for processing. Processing of model consists of domain creation, meshing, solver setting, boundary condition, solution initialization. Results and contours of solution were plotted in post-processor of ANSYS software. Flow Diagram of Methodology is shown in Figure 1.

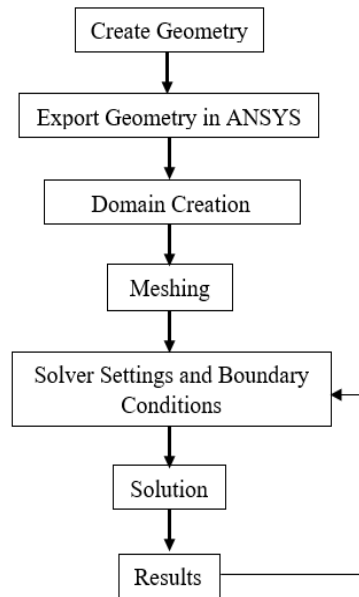


Fig. 1. Flow diagram

2.1 Modelling

Modelling of 81mm mortar was done according to the dimensions as shown in Figure 2 and Figure 3. The model contains four parts

- i. Fuze
- ii. Shell Body
- iii. Cartridge
- iv. Fin Set

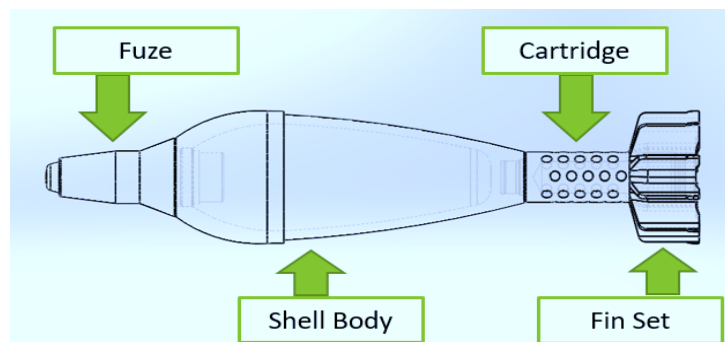


Fig. 2. 2D Drawing of 81mm mortar shell (French modified)

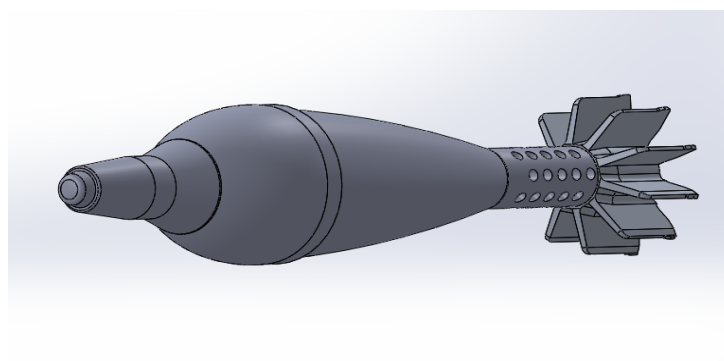


Fig. 3. 3D Model of 81mm mortar shell (French modified)

2.2 Domain Creation

Fluid domain was created in ANSYS which may be cylindrical or rectangular but it must be 15-20 times the target body (in length or area). Control volume's inlet, outlet and walls were defined here or it can be defined afterwards in Meshing. Fluid flow will be through the inlet of the control volume as shown in Figure 4.

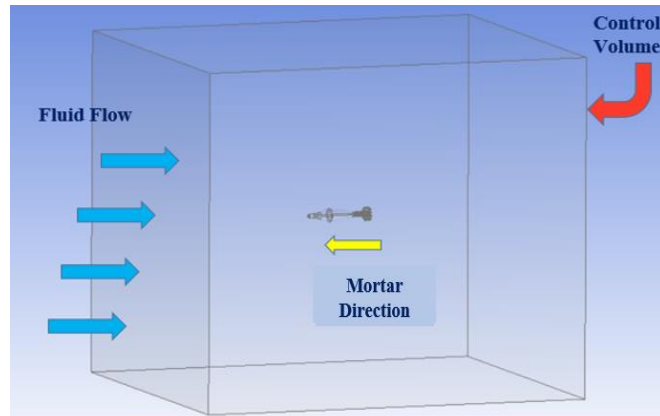


Fig. 4. Domain creation

2.3 Meshing

After geometry, the next step is meshing. For this, Mesh window of ANSYS was opened to generate auto mesh. After that mesh was fine-tuned manually with special considerations on fuze/face and edges/boundaries for getting accurate solutions/results as shown in Figure 5.

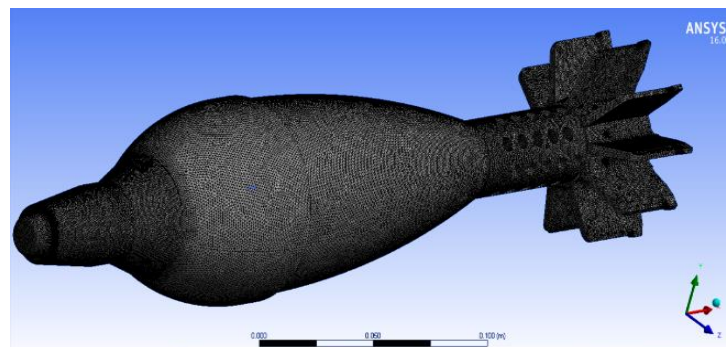


Fig. 5. Mesh on 81mm mortar shell (French modified)

2.4 Solver Settings and Boundary Conditions

After Mesh generation, the body with fluid domain is imported into ANSYS Fluent for processing. The next step is the selection of appropriate turbulence model. There are various turbulence models for solving a large number of problems. Viscous model selection is crucial. Reynolds Stress (RS) Model was chosen as the viscous models for turbulent flow problem.

After the selection of viscous model, boundary conditions were defined. In boundary conditions specifications, magnitude of velocity was defined. Magnitude of velocity should be changed for simulations at different Mach numbers. After the solution methods were defined/selected, the next step was to initialize the solution.

3. Results

The results of the analysis are given in Table 1 and Figure 6. Velocity Contour and Pressure Contour diagrams are shown in Figure 7 – Figure 12.

Table 1
Drag coefficient at different mach numbers

Mach Number	Velocity (m/s)	Coefficient of Drag
0.72	247	0.2093
0.76	261	0.2095
0.84	290	0.2099

From the given Table 1 and Figure 6 it was evident that there is a minor change observed in drag coefficient with an increase in Mach Number / air flow velocity and observed same till 10^{-3} .

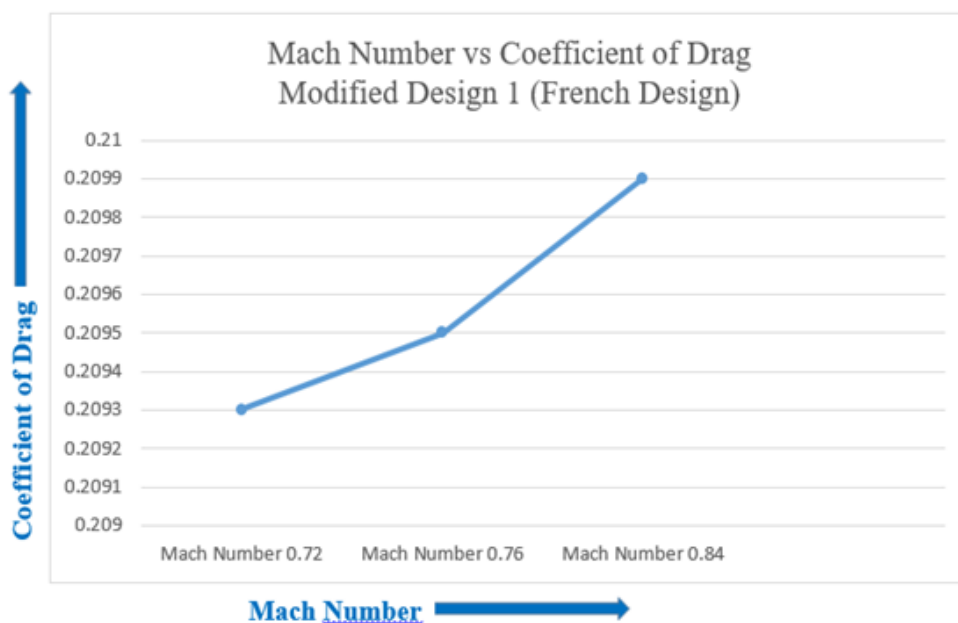


Fig. 6. Mach numbers vs. coefficient of drag

From Figure 7, 8 and 9 stagnation point was observed at fuze tip, as well as the velocity contour flowing from fuze tip to tail of motor shell increased till the maximum diameter observed at the foremost front of shell body are 2.786×10^2 , 3.057×10^2 and 3.397×10^2 respectively. After 1/3 of shell body length from the front, there is decrement in velocity observed which became more evident at 2/3 of the foresaid shell body length till the end of artillery shell.

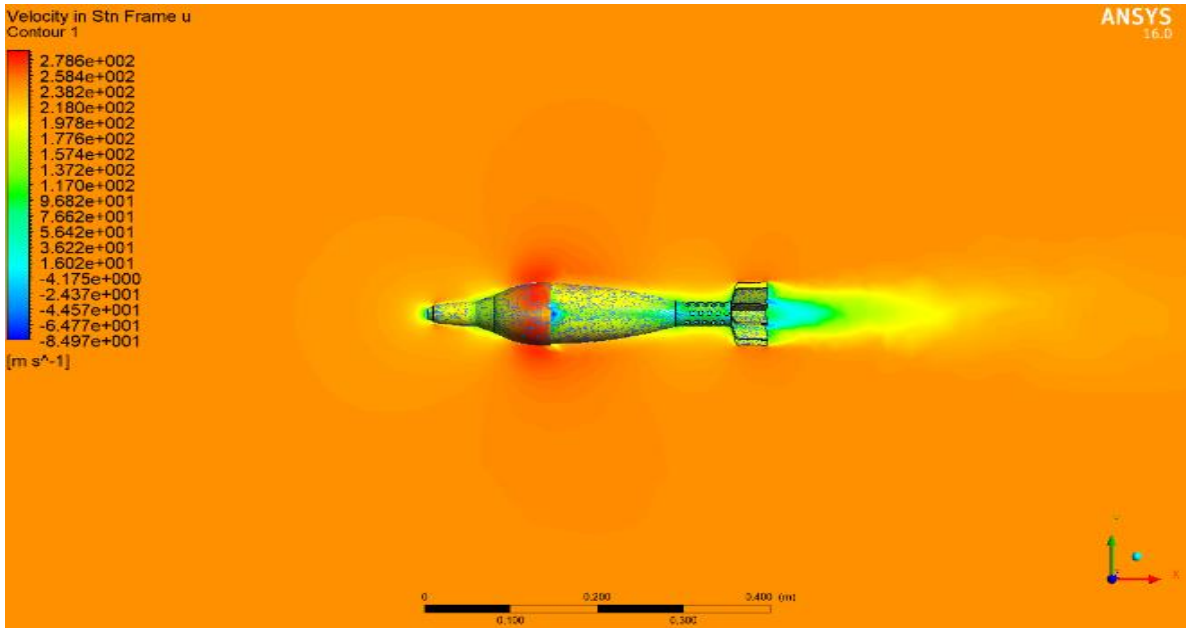


Fig. 7. Velocity contour of 81mm mortar shell (French modified) at mach number 0.72

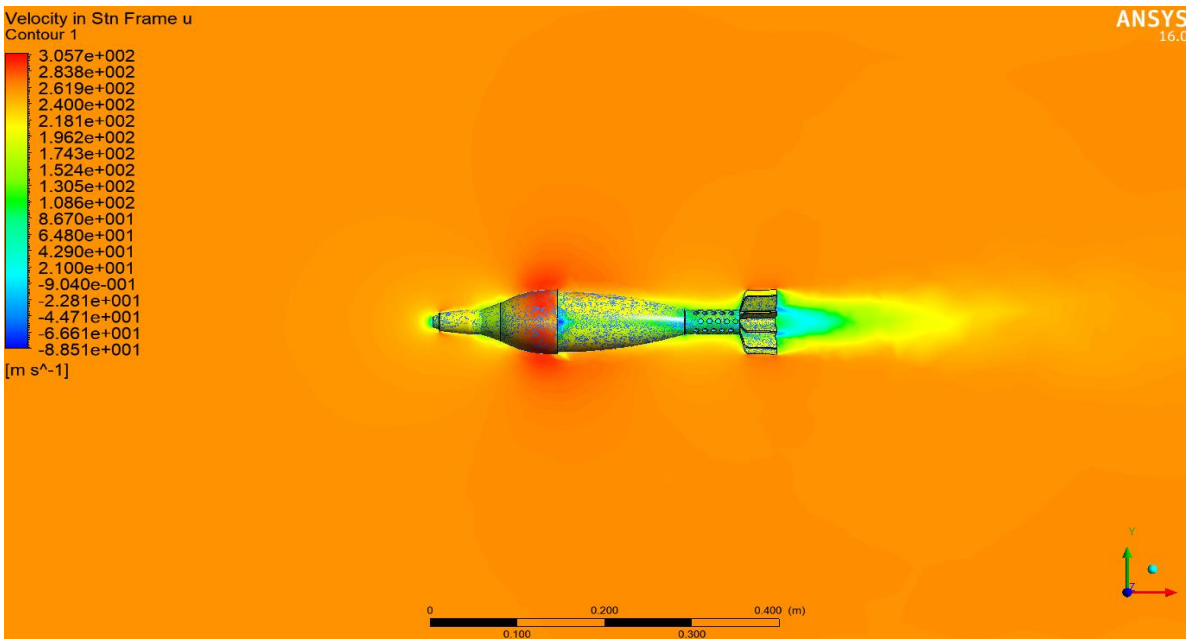


Fig. 8. Velocity contour of 81mm mortar shell (French modified) at mach number 0.76

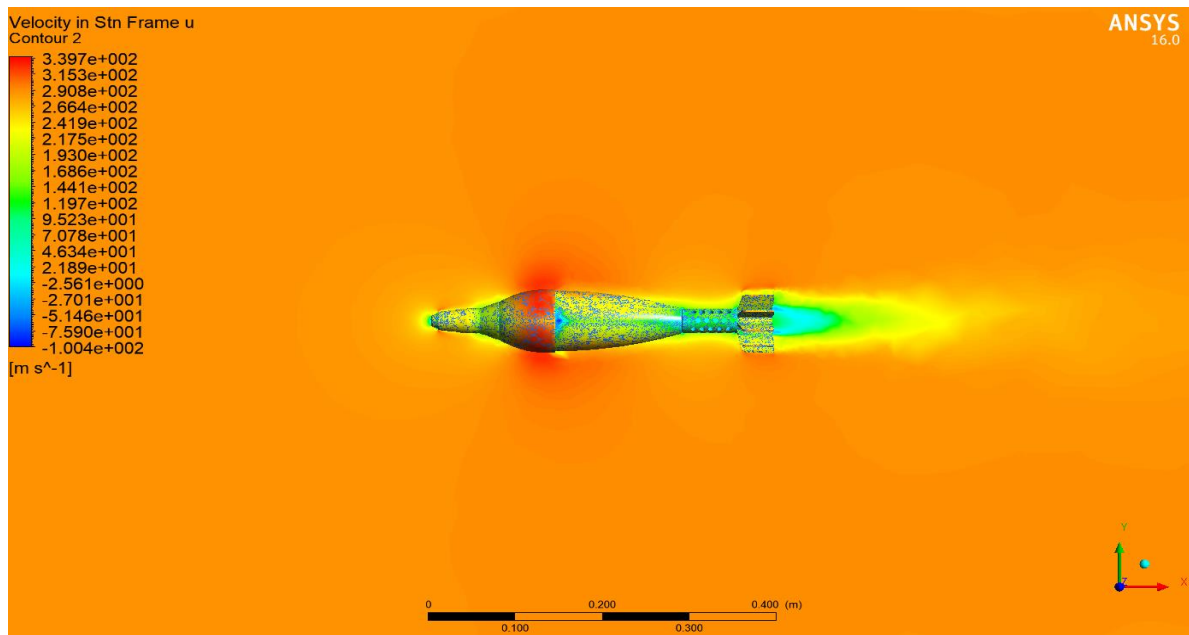


Fig. 9. Velocity contour of 81mm mortar shell (French modified) at mach number 0.84

From Figure 10, 11 and 12 stagnation point was observed at fuze tip as well as maximum pressure was observed due to minimum velocity at the fuze tip was 3.385×10^4 , 3.806×10^4 and 4.995×10^4 respectively which decrease till the maximum diameter of artillery shell and then again increases towards the cartridge case furthermore it decreases because of the air stream adverse interaction with artillery shell fins.

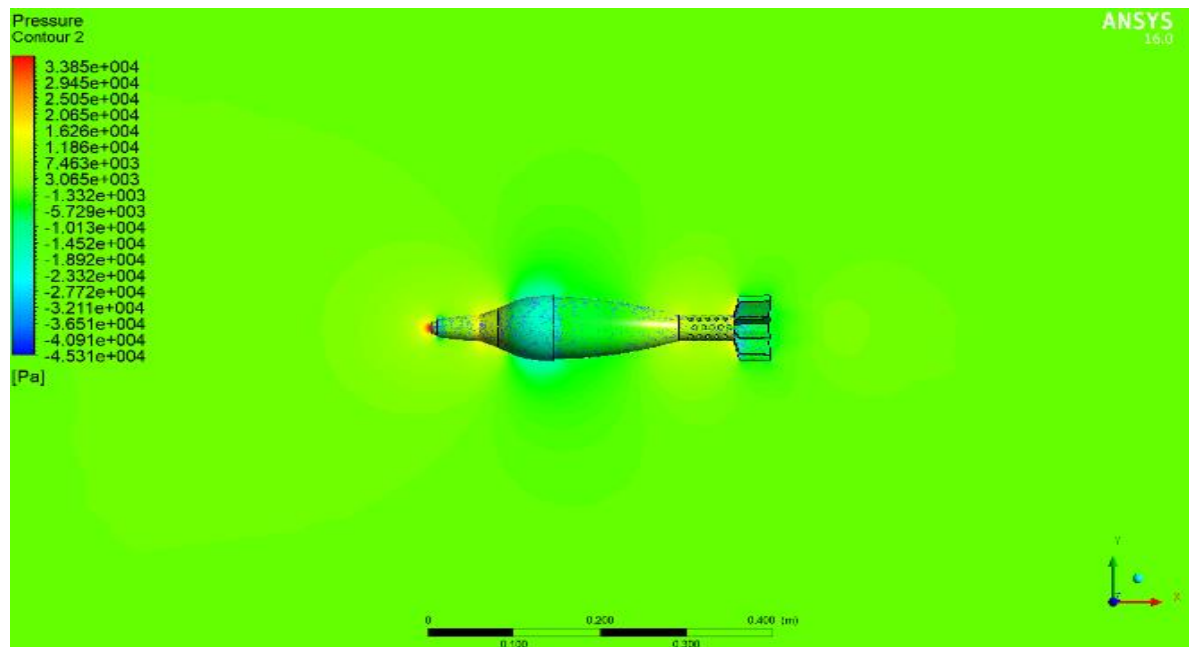


Fig. 10. Pressure contour of 81mm mortar shell (French modified) at mach number 0.72

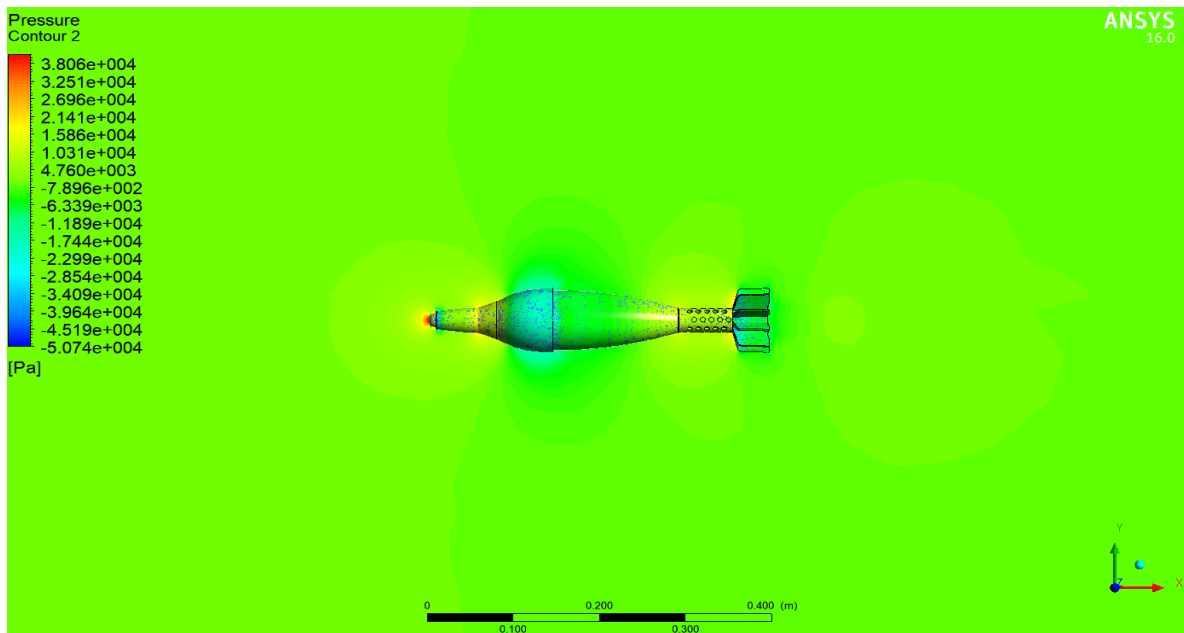


Fig. 11. Pressure contour of 81mm mortar shell (French modified) at mach number 0.76

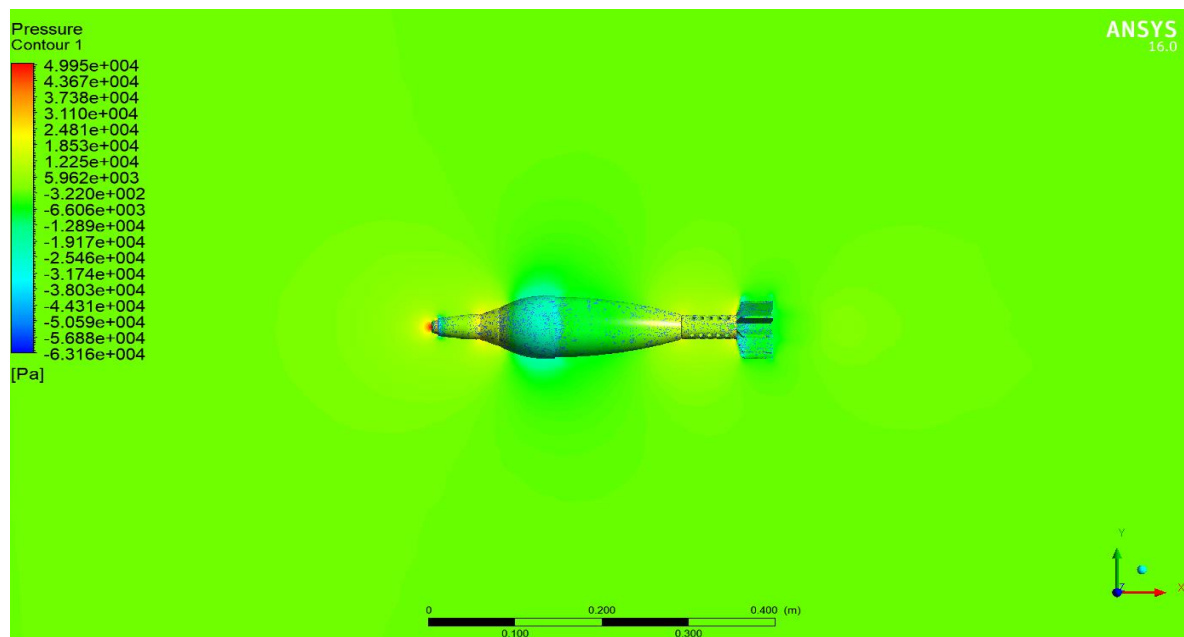


Fig. 12. Pressure contour of 81mm mortar shell (French modified) at Mach number 0.84

It was evident from velocity and pressure contours at various Mach numbers that separation starts at 1/3 of shell body length but became more evident at 2/3 of the shell body due to which pressure drag plays a vital role in producing drag coefficient value than that of foam drag.

4. Theoretical Range Calculation

In order to calculate the range of mortar shell, the formula for the range of unguided projectiles is given in a research paper named as “Development of Universal Trajectory Calculation Method for Unguided Projectiles” published by “Technical and Project Management Department of Turkish Land Forces Command” in the year 2004 [4] which is given below

$$\text{Range} = X = \{[9 t V \cos\theta \rho (K/2) + 1]^{(2/3)} - 1\} / 3\rho K$$

$$K = (C_d \times A) / (3m \times \cos\theta)$$

where,

X = Range (m)

t = Time of flight (s)

V = Launch velocity (m/s)

θ = Angle of launch (degree)

ρ = density of air (kg/m³)

K = Constant (m²/kg)

C_d = Coefficient of drag

A = Maximum area (m²)

m = Mass of mortar (kg)

In order to calculate “ ” for 81mm Mortar Shell (French Design) we have,

$$C_d = 0.2096$$

$$A = 3.14 (0.081)^2 \\ = 0.005153 \text{ m}^2$$

$$m = 2.528 \text{ kg}$$

$$\theta = 45^\circ$$

As,

$$K = (C_d \times A) / (3m \times \cos\theta)$$

$$K = (0.2096 \times 0.005153) / [3 \times 2.528 \times \cos(45^\circ)]$$

$$K = 0.0002014040012 \text{ m}^2/\text{kg}$$

Now, In order to calculate “Range (X)” for 81mm Mortar Shell (French Design) we have,

$$t = 35 \text{ s}$$

$$V = 319 \text{ m/s}$$

$$\theta = 45^\circ$$

$$\rho = 1.225 \text{ kg/m}^3$$

$$K = 0.0002014040012 \text{ m}^2/\text{kg}$$

As,

$$\text{Range} = X = \{[9 t V \cos\theta \rho (K/2) + 1]^{(2/3)} - 1\} / 3\rho K$$

$$X = \frac{[9 \times 35 \times 319 \times \cos(45^\circ) \times 1.225 \times \frac{0.0002014040012}{2} + 1]^{2/3} - 1}{3 \times 1.225 \times 0.0002014040012}$$

$$X = 4821.44097 \text{ m}$$

So,

Theoretical Range = 4821.44097 m

81mm Mortar Shell (French Modified)

Existing Range = 4550 m

Existing Design

Enhanced Range of Mortar = 4821 – 4550
= 271 m

5. Conclusions

Firing test results of original model were compared and validated with CFD results occupied through ANSYS Fluent 16.0. The drag coefficient of 81mm Mortar Shell (French Design) is found to be less than that of existing one. Low coefficient of drag results in enhanced range of mortar shell. The range of mortar shell is increased by 271 meters because of low drag coefficient with 5.96% percent increase in range and 15.73% decrease in drag coefficient value. The new design is feasible and more efficient than that of the existing one for production. Parabolic type fuze would furthermore results of an increase in aerodynamics, range enhancement and drag coefficient reduction but in terms of setup change it would be a major concern due to complexity of fuze mechanism.

It was evident from velocity and pressure contours at various Mach numbers that separation starts at 1/3 of shell body length but became more evident at 2/3 of the shell body due to which pressure drag plays a vital role in producing drag coefficient value than that of foam drag. Furthermore from the CFD experimentation it was also observed that the drag due to fuze and fins plays a vital role in producing drag coefficient but not that much which was produced due to early separation of air flow stream at the shell body. So thereby it was concluded that further research should be carried out on shell body to delay separation and thereby reducing drag coefficient and increasing artillery shell range. Also change in shape of shell body would be more suitable for change in manufacturing setup in future instead of changing fuze and fins that have a complex design and mechanism as compared to shell body.

References

- [1] Boyer, Eugene D. *Aerodynamic Properties of 60-MM Mortar Shell, T24*. ARMY BALLISTIC RESEARCH LAB ABERDEEN PROVING GROUND MD, 1956. <https://doi.org/10.21236/AD0107138>
- [2] Odom, Charles T. *A DRAG COEFFICIENT, KD, BASED ON 155MM SHELL, HE, M101*. ARMY BALLISTIC RESEARCH LAB ABERDEEN PROVING GROUND MD, 1958. <https://doi.org/10.21236/AD0209134>
- [3] STUREK, WALTER, and CHARLES NIETUBICZ. "Recent applications of CFD to the aerodynamics of army projectiles at the US Army Ballistic Research Laboratory." In *Guidance, Navigation and Control Conference*, p. 4349. 1992. <https://doi.org/10.2514/6.1992-4349>
- [4] Akçay, Mehmet. "Development of universal flight trajectory calculation method for unguided projectiles." *Turkish Journal of Engineering and Environmental Sciences* 28, no. 6 (2004): 369-376.
- [5] Damljanović, Dijana, Slobodan Mandić, and Đorđe Vuković. "Computational fluid dynamics and wind tunnel determination of the aerodynamic characteristics of an axi-symmetric projectile with a conical tail flare." *Scientific Technical Review* 61, no. 3-4 (2011): 49-55.
- [6] Sagat, Chandrakant, Pravin Mane, and B. S. Gawali. "Experimental and CFD analysis of airfoil at low Reynolds number." *International Journal of Mechanical Engineering and Robotics Research* 1, no. 3 (2012): 277-283.
- [7] Li, Chun Chi, Chang Sheng Tai, Cheng Chyuan Lai, Shang Min Fu, and Yen Chun Tsai. "The Aerodynamic Attributes and Flight Trajectories of a Tail Fin-Stabilized Projectile." In *Applied Mechanics and Materials*, vol. 415, pp. 544-547. Trans Tech Publications Ltd, 2013. <https://doi.org/10.4028/www.scientific.net/AMM.415.544>
- [8] Parab, Akshay, Ammar Sakarwala, Bhushan Paste, Vaibhav Patil, and Amol Mangrulkar. "Aerodynamic analysis of a car model using Fluent-Ansys 14.5." *International Journal of Recent Technologies in Mechanical and Electrical Engineering (IJRMEE) Volume 1* (2014): 2349-7947.

- [9] Hassan, SM Rakibul, Toukir Islam, Mohammad Ali, and Md Quamrul Islam. "Numerical study on aerodynamic drag reduction of racing cars." *Procedia Engineering* 90 (2014): 308-313. <https://doi.org/10.1016/j.proeng.2014.11.854>
- [10] Li, Chun-Chi, Chang-Sheng Tai, Cheng-Chyuan Lai, Shang-Min Fu, and Yen-Chun Tsai. "Study of the aerodynamic characteristic and flight trajectories in a tail fin-stabilized projectile with different shapes." *Procedia Engineering* 79 (2014): 108-113. <https://doi.org/10.1016/j.proeng.2014.06.317>
- [11] Doig, Graham, Shibo Wang, Harald Kleine, and John Young. "Aerodynamic analysis of projectiles in ground effect at near-sonic mach numbers." *AIAA Journal* 54, no. 1 (2016): 150-160. <https://doi.org/10.2514/1.J054114>
- [12] Chaurasiya, Vikas V., Deepak B. Kushwaha, and Mohd Raees. "Aerodynamic analysis of vehicle using CFD." *International Journal of Recent Trends in Engineering & Research* 3, no. 3 (2017): 131-137. <https://doi.org/10.23883/IJRTER.2017.3056.S0SEM>
- [13] Fedaravicius, Algimantas, Valenza Francesco, Arvydas Survila, and Minvydas Ragulskis. "Development of the Mortar Simulator and Estimation of the Drag Force Acting to the Warhead." *Recent Advances in Mechanical Engineering and Automatic Control*: 110-114.
- [14] Sahu, Jubaraj, and Karen R. Heavey. "Advanced computational fluid dynamics simulations of projectiles with flow control." In *SC'04: Proceedings of the 2004 ACM/IEEE Conference on Supercomputing*, pp. 27-27. IEEE, 2004.
- [15] Zhang, Chengqing, Huiyuan Wang, Pengjun Zhang, Shuhua Gao, and Hao Xiong. "CFD simulation of a finned smart bullet with microactuator." In *Journal of Physics: Conference Series*, vol. 1064, no. 1, p. 012021. IOP Publishing, 2018. <https://doi.org/10.1088/1742-6596/1064/1/012021>